One-bond 1J(15N,H) coupling constants at sp2 hybridized nitrogen of Schiff bases, enaminones and similar compounds. A theoretical study.

Hansen, Poul Erik; Saeed, Bahjat Ali; S. Elias, Rita; Kupka, Teobald

Published in:
Magnetic Resonance in Chemistry

DOI:
10.1002/mrc.5052

Publication date:
2020

Document Version
Peer reviewed version

Citation for published version (APA):
Hansen, P. E., Saeed, B. A., S. Elias, R., & Kupka, T. (2020). One-bond 1J(15N,H) coupling constants at sp2 hybridized nitrogen of Schiff bases, enaminones and similar compounds. A theoretical study. *Magnetic Resonance in Chemistry*, *58*(8), 750–762. https://doi.org/10.1002/mrc.5052

Hansen Poul Erik (Orcid ID: 0000-0003-4751-9910)

Saeed Bahjat (Orcid ID: 0000-0002-0288-5389)

Kupka Teobald (Orcid ID: 0000-0002-6102-0158)

One-bond $^{1}J(^{15}N,H)$ coupling constants at sp^2 hybridized nitrogen of Schiff bases, enaminones and similar compounds. A theoretical study

Poul Erik Hansen[1*], Bahjat A. Saeed[2], Rita S. Rutu[3] and Teobald Kupka[4*]

[1]Department of Science and Environment, Roskilde University, P.O.Box 260, DK-4000 Roskilde, Denmark; [2] Department of Chemistry, College of Education for Pure Sciences, University of Basrah, Iraq; [3]Department of Pharmaceutical Chemistry, College of Pharmacy, University of Basrah, Iraq; [4]University of Opole, Faculty of Chemistry, 45-052 Opole, Poland

Abstract

$^{1}J(^{15}N,H)$ coupling constants for enaminones and NH-forms of intramolecularly hydrogen bonded Schiff bases as model compounds for sp^2 hybridized nitrogen atoms are evaluated using density functional theory (DFT) to find the optimal functionals and basis sets. Ammonia is used as a test molecule and its one-bond coupling constant is compared with experiment. A methyl amine Schiff base of a truncated molecule of gossypol is used for checking the performance of selected B3LYP, O3LYP, PBE, BHandH and APFD density functionals and standard, modified and dedicated basis sets for coupling constants. Both in vacuum and in chloroform, modeled by the simple continuum model of solvent, the modified basis sets predict significantly better the $^{1}J(^{15}N,H)$ value in ammonia and in the methyl amine Schiff base of a truncated molecule of gossypol than the standard basis sets. This procure is then used on a broad set of intramolecularly hydrogen bonded molecules and a good correlation between calculated and experimental one bond NH coupling constants is obtained. The $^{1}J(^{15}N,H)$ couplings are slightly overestimated. The calculated data show for hydrogen bonded NH interatomic distances that the calculated values depend on the NH bond lengths. The shorter the bond lengths, the larger the $^{1}J(^{15}N,H)$. A useful correlation between $^{1}J(^{15}N,H)$ and NH bond length is derived that enables realistic predictions of one bond NH coupling constants. The calculations reproduce experimentally observed trends for the studied molecules.

Keywords: DFT calculations, One-bond NH coupling constants, Schiff bases, NH-forms, SSCC, Tautomerism

This article has been accepted for publication and undergone full peer review but has not been through the copyediting, typesetting, pagination and proofreading process which may lead to differences between this version and the Version of Record. Please cite this article as doi: 10.1002/mrc.5052

Corresponding Author: Poul Erik Hansen - Department of Science and Environment, Roskilde University, P.O.Box 260, DK-4000 Roskilde, Denmark, Fax +45 46743011; E-mail: poulerik@ruc.dk and
Teobald Kupka - University of Opole, Faculty of Chemistry, 45-052 Opole, Poland, orcid.org/0000-0002-6252-3822; Email: teobaldk@gmail.com

1. INTRODUCTION

$^{1}J(^{15}N,H)$ indirect spin-spin coupling constants (SSCC) have been used extensively to estimate mole fractions for tautomeric systems such as Schiff bases of *o*-hydroxyacyl aromatics and salicylaldehydes[1-6] (see **Fig. 1**).

They have been measured in a few cases in enaminones.[7-8] However, one of the problems of using $^{1}J(^{15}N,H)$ in studies of Schiff bases is that very few have been determined for compounds fully at the NH-form.[9-10] $^{1}J(^{15}N,H)$ has typically been estimated using model compounds such as enaminones[5, 7-8] or even hydrazones[11]. Some general observations have been made. One-bond coupling constants can be correlated to the bond order of the N-H bond[12]. The larger the bond order, the larger $^{1}J(^{15}N,H)$. It has also been observed that $^{1}J(^{15}N,H)$ increases when going from RNH_2 to RNH_3^+. In protonated imines the $^{1}J(^{15}N,H)$ are ~ 92 Hz[13]. A similar value was found by Kurkovskaya et al.[14] for protonated Schiff bases. A number of generalizations have been obtained from ammonia and aliphatic amines regarding influence of bond angles, etc. As these apparently relate to pyrimidality[15], they are not so relevant in the present compounds. Solvent effects have also been studied and showed for anilines a larger value in DMSO than in $CDCl_3$.[16] For enaminones Dudek and Dudek[5] found that $^{1}J(^{15}N,H)$ coupling constants vary with the substituent at nitrogen. Variations in $^{1}J(^{15}N,H)$ of Schiff bases have been discussed.[17] These variations could be linked to the substituents and indirectly to the balance between charged and non-charged resonance forms.

Previously, $^{1}J(^{15}N,H)$ coupling constants have been calculated for Schiff bases on salicylaldehydes.[18] The functional used was B3LYP in combination with cc-pVTZ basis set for O, N, C7 and H1 and 6-31G** for other carbon and hydrogen atoms. A rather peculiar behaviour is seen with a numerical increase of $^{1}J(^{15}N,H)$ for short NH bond and then a decrease upon bond stretching after ~1.1Å.

Currently organic chemists are seeking fast answers supporting understanding of their experiments.[19] The Gaussian program package[20] has been known as a user-friendly and handy tool for people without deep inclination to theoretical chemistry. Thus, it is possible to easily predict nuclear shieldings and chemical shifts[21] by selecting a density functional[22-23] (say B3LYP[24-26]) and a medium size Pople-type basis set[27-28] without special knowledge. However, in case of coupling constants some knowledge about the basis set nature is necessary[29-30] and a danger of

treating the Gaussian program as a “black box” is real. It is generally accepted that modeling SSCC parameters[31], which are absolute numbers, is significantly more demanding computationally than predicting reliable isotropic nuclear magnetic shieldings and chemical shifts (the latter are relative values). This is partly due to cancellation of similar errors included in the shieldings of the molecule of interest and the reference. The second reason is the need to correctly model electronic density near, and at the nuclei by using dedicated basis sets containing tight s-functions.[29, 32-33] Thus, reliable prediction of SSCC parameters require dedicated basis sets[30, 32-33] which are fairly large and sometimes impractical for studies on medium size molecules.

In the Gaussian 16 program package[20] a “mixed[35]” option of basis set is available which significantly improves on the quality of the predicted SSCC. According to Ramsey[36], the total indirect spin-spin coupling constant consists of four terms – Fermi contact term (FC), spin-dipole (SD), diamagnetic spin-orbit (DSO), and paramagnetic spin-orbit (PSO). In short, in the first step of mixed approach the FC term is evaluated using mixed option by an uncontracted basis set and with added tight polarization functions for the core. The remaining three terms are calculated with an unmodified basis set. As a result, the total SSCC value is significantly improved. In addition, the entire calculation is faster. Thus, for a less experienced user the Gaussian offers a simple approach, allowing reasonable calculation of SSCC parameters without searching for basis sets dedicated for coupling constants.

In principle, one-bond CH couplings (SSCC) can be calculated quite well using large, dedicated basis sets.[30-31, 37-38] The use of DFT functionals for predicting NMR parameters have been reviewed.[37, 39-40] One-bond C-H couplings and their dependence on basis set and functionals have recently been investigated and it has been shown that even for specially designed large basis sets containing tight functions, both shifting (scaling), correlations, as well as inclusion of solvent effects and zero-point rovibrational corrections (ZPVC) may be necessary to obtain good results[37, 40-41]. For $^{1}J(^{15}N,H)$ couplings B3LYP functionals worked fairly well with modified Dunning’s aug-cc-pVTZ-J triple-ζ basis set[33, 42].

Frisch et al.[35] tested the prediction of $^{1}J(^{14}N,H)$ coupling constant in ammonia and several small molecules in the gas phase. Other authors also reported calculations on ammonia coupling between the more abundant nitrogen isotope (^{14}N) and

hydrogen[31, 43]. The question is if the rigorous approach for estimation of accurate $^1J(^{14}N,H)$ and $^1J(^{15}N,H)$ coupling constants[44-46] can be applied to medium size molecules in nonpolar solvent and in the presence of intramolecular hydrogen bonding.

The aim of the present study is to calculate $^1J(^{15}N,H)$ in a series of *medium* size organic compounds with sp^2 hybridized nitrogen to generalise some of the above mentioned single observations made for enaminones and to provide a way of predicting $^1J(^{15}N,H)$ in NH-forms of tautomeric compounds like Schiff bases. $^1J(^{15}N,H)$ is well known to be negative. As the sign of the coupling constants is not so easy to be determined experimentally, only numerical values are dealt with in plots.

The present investigation focuses on a range of small to medium size compounds having NHR groups in different functionalities, as depicted in **Fig. 1,** and on hydrogen bonding. B3LYP functional has been shown to perform well for small sets of compounds[43, 47] and for intramolecularly hydrogen bonded molecules. However, for more reliable prediction of $^1J(^{15}N,H)$ in medium size molecules we decided to test the performance of several density functionals and basis sets. In the first step we used ammonia as a small molecule, suitable for fast modelling using fairly large basis sets. In particular, we wanted to check the option “mixed”, producing a de-contraction of a standard basis set, recently available in the Gaussian programs[20] and compare their performance with dedicated Jensen-type basis sets pcJ-2[32] and aug-pcJ-n[32], where n = 1, 2, 3 and 4. In the second step we tested the performance of selected density functionals and basis sets for prediction of $^1J(^{15}N,H)$ of the demanding methylamine Schiff base of 2,3,8-trihydroxy-7-methyl-1-napthaldehyde (see **Fig. 1 F and Fig. 2a**) in the following called MSBTG and the results were critically compared with available experimental data. Finally, we applied the optimized selection of density functional and basis sets on several compounds (**Table 1**) with internally bonded N-H…O motif.

2. EXPERIMENTAL

2.1. Data

Experimental data are taken from literature. Difficulties are related to the fact that one has to take into account the exchange of the NH proton. However, to solve this problem some results have been checked at a range of temperatures. Another issue is tautomeric. Again, temperature studies are very useful. In case of tautomeric compounds derived from aldehydes, a three-bond coupling from NH, the CH of 12.5 Hz is a check of the shift of the equilibrium fully to the NH form. One issue about using lower temperatures is the possible variation of $^{1}J(^{15}N,H)$ with temperature. However, this has not been studied systematically, but the results for **3**, 5,5-dimethyl-3-methylaminocyclohex-2-en-1-one and **10** indicates that $^{1}J(^{15}N,H)$ may decrease 0.3 Hz when changing the temperature from 304 to 245 K.[48] On the other hand this is not the case for **3** and **11** for which no temperature effect was observed. For the molecules **3** and **11** a change in $^{1}J(^{15}N,H)$ in $CDCl_3$ vs. CCl_4 of ~0.7 Hz is found. This is a very large change considering the similarity of the two solvents.

2.2. Computational part

Molecular geometries were optimised using the Gaussian 16 suite of programs[20]. Density functional theory, combined with widely used and efficient B3LYP hybrid functional (Becke's[24] exchange and Lee, Yang, Parr[25] correlation term) and 6-311++G(d,p) basis set were used for full structure optimization using very tight convergence criteria. Unrestricted geometry optimization and NMR calculations at selected levels of theory were done either in the gas phase or using the IEFPCM[50] approach in the presence of $CHCl_3$ solvent. The SSCC parameters were calculated using the keyword NMR(spinspin,mixed,readatom) for standard basis sets in mixed form and NMR(spinspin,readatom) for basis sets dedicated for SSCC calculation with five selected density functionals (B3LYP[24-26], O3LYP[51], PBE[52-53], BHandH[54] and APFD[55]) and several basis sets. Ammonia was used as a test molecule for studying the impact of standard and decontracted Pople-type basis sets 6-31G* and 6-311++G**. In addition, aug-cc-pVTZ-J[29, 33, 56-59] (abbreviated as aVTZJ), and polarization-consistent basis sets designed for SSCC calculations (pcJ-2[32] and aug-pcJ-n_2006[60], where n = 1 - 4) were used for predicting ammonia $^{1}J(^{15}N,H)$. The

basis sets dedicated for prediction of SSCC parameters were downloaded from the basis set exchange (EMSL[61-62]) and, for convenience, were abbreviated as pcJ2 and apcJn. To avoid recalculation of coupling constants from the most abundant ^{14}N isotope to $^{1}J(^{15}N,H)$, in the input z-matrix we used N(Iso = 15) entry. For the results obtained with aug-pcJ-n_2006 basis sets the CBS[43, 63-67] fit, using two-parameter formula,[43, 68] was performed. For correlation-consistent basis sets (cc-pVXZ[69-71]), X = D, T, Q, 5 and 6 and the smallest basis, X = D, corresponds to double-zeta quality. However, for pcJ-n basis set family, where n = 0,1,2,3 and 4, the parameter n = 1 already corresponds to the double-zeta quality.[32, 72-73] Thus, for consistency, all fittings for Dunning type basis sets were performed against X = 2,3,4,5 and 6, and for aug-pcJ-n_2006 basis sets we used a value of X = n + 1. Obviously, the smallest basis sets produce least accurate results. Thus, to assure estimation of meaningful results, fittings were performed with regularly changing basis set size, using n = 2, 3 and 4, written as CBS(2-4), or only 3 and 4 (abbreviated as CBS(3,4)). A truncated version of gossypol molecule (called here MSBTG) has been used (**Fig. 2**). Gossypol exists as dimer but the truncated form MSBTG (**a** of Fig. 2**)** has been used as this give a B3LYP calculated coupling constant of $^{1}J(N,H)_{calc}$ = -90.69 Hz, which is similar to that of form **b**, $^{1}J(N,H)_{calc}$ = -90.48 Hz. The former can be considered a good model for a Schiff base of gossypol. A Schiff base of gossypol has been chosen as it shows extra hydrogen bonding, a large, conjugated aromatic system and a steric strain and should as such cover a large group of compounds. Furthermore, the Schiff base of gossypol is one of the few aromatic Schiff bases fully at the imine form.[9] MSBTG molecule optimized in chloroform at B3LYP/6-311++G(3df,2pd) level of theory was used as input for SSCC calculations with B3LYP and BHandH[54] density functionals in vacuum and in chloroform using standard and “mixed” versions of 6-31G*, 6-311++G** and 6-311++G(3df,2pd) basis sets, as well as standard pcJ-2 one. All the studied molecules were finally modeled using B3LYP/6-311++G** structures optimized in chloroform, and the subsequent SSCC parameters were predicted using APFD density functional[55]. These calculations were performed with APFD/6-311++G**(mixed) approach in $CHCl_3$.

3. RESULTS and DISCUSSION

3.1. Prediction of $^{1}J(^{15}N,H)$ in ammonia

Ammonia was selected as the first molecule for testing selected density functionals performance in predicting $^{1}J(^{15}N,H)$ indirect coupling constant in vacuum and in chloroform, modeled by polarized continuum model of solvent and using selected traditional (standard) Pople type basis sets and "mixed" ones, created by Gaussian 16. Comparison of the predicted ammonia SSCC coupling constant, observed for ^{15}N NMR spectrum in the gas phase (-61.47±0.02 Hz[74]) should include correction for zero-point vibration (1.33[43] Hz for $^{1}J(^{14}N,H)$ and -0.3[45] or 0.3[46] Hz for $^{1}J(^{15}N,H)$). However, in the current study we will not include these fairly small corrections since calculation of ZPVC is very expensive and for our medium size molecules practically impossible. It is also important to mention that solvent effect in case of ammonia $^{1}J(^{15}N,H)$ is fairly small (see discussion in refs. [74-75]).

To see the impact of geometry, the ammonia structure was first calculated in vacuo at B3LYP/6-311++G** level of theory. The B3LYP predicted SSCC values for the isolated ammonia molecule in the gas phase, obtained with 6-311++G** and 6-311++G**(mixed) basis sets were -59.072 and -64.478 Hz, respectively. The presence of chloroform caused only minute change in the optimized structural parameters. As result, these SSCC values also changed only slightly (-60.210 and -65.713 Hz). Thus, the former SSCC values, obtained with standard basis sets, were more positive by about 5.5 and 5.4 Hz than the latter results, obtained with the mixed option in the gas phase and chloroform, respectively.

Next, five arbitrary selected density functionals, including B3LYP, O3LYP, PBE, BHandH and APFD, were used to optimize NH_3 molecule in vacuum and in chloroform, using the standard 6-311++G** basis set. Subsequent SSCC predictions in vacuum and chloroform were calculated with 6-311++G**(mixed) variant of the original Pople-type basis set. For brevity, the calculated values are gathered in **Table S1** in the supplementary material and in **Fig. 3** the $^{1}J(^{15}N,H)$ values of ammonia in the gas phase and in chloroform, calculated with 6-311++G**(mixed) basis set, are compared with experimental values.

It is apparent from the above results that both in vacuum and in chloroform the SSCC values, calculated with these density functionals, differ by about 5 Hz or less. Interestingly, the PBE and APFD density functionals nicely reproduce experimental

value of ammonia one-bond $^{1}J(^{15}N,H)$ coupling constant in chloroform (within 0.5 Hz).

Since ammonia is a very small molecule, we decided to check the performance of selected dedicated basis sets aug-cc-pVTZ-J and aug-pcJ-n_2006, where n = 1, 2,3 and 4, for predicting $^{1}J(^{15}N,H)$ in chloroform and compare the results with relatively small, standard and mixed Pople basis set 6-311++G** (see **Fig. 4,** as well as **Table S2** in the supplementary material). The data obtained with a family of aug-pcJ-n_2006 basis sets were used for estimation of the CBS values of the studied coupling constant using two-parameter fits (**Table S2** and **Fig. S1**).

It is evident from **Fig. 4** that the original 6-311++G** basis set is inaccurate in prediction of experimental values of $^{1}J(^{15}N,H)$ in ammonia and its mixed version performs fairly close to the dedicated basis sets (the latter values are systematically more negative by about 4-6 Hz). Interestingly, both PBE and APFD produce the best agreement with experimental value for both 6-311++G**(mixed) and dedicated basis sets.

In addition, starting from results obtained with aug-cc-pVTZ-J basis set, the couplings are overestimated and their values are practically converged within 1 Hz. This is also supported by the estimated CBS values (see **Table S2 and Fig. S1**). Thus, from **Table S2** it is evident that the $^{1}J(^{15}N,H)$ value in ammonia calculated with mixed Pople-type basis set is close to the result, derived at the complete basis set limit and is within 2 Hz from experimental values for O3LYP, PBE and APFD. Somehow, larger deviations (about 4-6 Hz) are observed for B3LYP and BHandH.

3.2. *Prediction of $^{1}J(^{15}N,H)$ in MSBTG*

It is known that general basis sets are not suitable for calculations of SSCC because the dominating FC component is poorly recovered. However, the accuracy of calculation could depend on the type of nuclei taking part in coupling, as well as molecular surrounding of the studied spins and separation between them. To get a direct insight into the composition of the total SSCC (J_{tot}), we present in **Table S3** in the supplementary material MSBTG's total $^{1}J(^{15}N,H)$ coupling and its four components, calculated with B3LYP density functional in the gas phase and chloroform, with standard and mixed 6-31G* and 6-311++G** basis sets using

geometries optimized with the same density functional and standard basis sets in both environments.

The composition (in %) of MSBTG's $^{1}J(^{15}N,H)$ individual components, calculated in the gas phase and chloroform using two basis sets, is shown in **Table 2**. Looking at **Table 2** it is obvious that the dominating component of $^{1}J(^{15}N,H)$ calculated with standard and mixed basis sets is FC (about 98%) and the SD, DSO and PSO terms are very small.

From the results gathered in **Table S3** it is obvious that the mixed basis set recovers a higher absolute amount of the FC component. Besides, using two different basis sets the optimized structures of MSBTG were slightly different (data not shown here) and the calculated coupling constants were negligible smaller in chloroform.

In **Table 3** are gathered $^{1}J(^{15}N,H)$ coupling constants for MSBTG calculated as an isolated molecule in the gas phase and in chloroform, modeled by the PCM method, using B3LYP density functional and mixed versions of three popular Pople-type basis sets.

In this case geometry is calculated with standard 6-31G*, 6-311++G** and 6-311++G(3df,2pd) basis sets in the gas phase and chloroform and next SSCCs are calculated with mixed options of the same basis sets and compared with the experimental value.

It is apparent from **Tables 2** and **3** that optimization of an isolated MSBTG molecule in the gas phase or in chloroform and subsequent calculation of the one-bond nitrogen-proton coupling constant at the same level of theory improves only negligible the agreement with experiment upon including solvent effect (deviation of 0.1 to 0.4% between results in vacuum and solution). Upon improving the basis set from 6-31G* to 6-311++G** the calculated coupling decreases by about 1.1 to 1.3 Hz in the gas phase and chloroform (< 1.5%). Thus, as expected, geometry seems to be less important for prediction of MSBTG $^{1}J(^{15}N,H)$ coupling. However, we further wanted to check, if markedly better basis set produce significantly different couplings. First, we optimized MSBTG structure in chloroform at B3LYP/6-311++G(3df,2pd) level of theory. Next, apart from B3LYP, we included BHandH density functional and pcJ-2 basis set in the test in chloroform. The choice of BHandH was justified by our earlier experiences with this density functional[76], in

calculations of both isotropic shieldings and SSCC parameters of H_2O, H_2, HF, F_2 and F_2O. The obtained SSCC parameters are shown in Table **4**. Surprisingly, the best performance is observed for the smallest basis set (6-31G*). However, we are aware that this could be due to favourable error cancellation. In addition, the dedicated Jensen basis set (pcJ-2) produces the largest deviation from experiment. Since this basis set is known to produce results close to the complete basis set limit (CBS) we could assume that the observed deviations for B3LYP and BHandH of about 8.4% are intrinsic errors of these density functionals (compare CBS results produced by these density functionals in ref. [43]). It is also apparent that 6-311++G**(mixed) basis set produce relatively small deviations (about 7.1%) and is fairly complete and flexible for reliable calculations of $^1J(^{15}N,H)$ parameters of medium size molecules.

In the next step we compared the performance of B3LYP and APFD density functionals in prediction of MSBTG $^1J(^{15}N,H)$ coupling constant using the standard 6-311++G** basis set and its mixed variant with the results produced by dedicated basis sets pcJ-2 and aug-pcJ-2_2006 in the presence of $CHCl_3$ (**Table 5**). As before, the geometry was optimized at the B3LYP/6-311++G(3df,2pd) level of theory in chloroform. Interestingly, B3LYP and APFD calculations with the dedicated basis set pcJ-2 produced fairly large deviations from experimental values (-7.46 and -2.69 Hz). However, the corresponding numbers decreased in case of 6-311++G**(mixed) basis set (-6.34 and -1.65 Hz). The latter result could indicate a very good performance of this modified basis set combined with the APFD density functional. However, upon improving the quality of basis set to aug-pcJ-2_2006, about two times worse result was obtained (-3.81 Hz). The data in **Table 5** suggest a significantly better performance of APFD than B3LYP in prediction of MSBTG $^1J(^{15}N,H)$ coupling constants and point out to a very practical level of calculations: APFD/6-311++G**(mixed). The computational cost is related to the number of basis functions and in case of the mixed Pople basis only the Fermi contact term is calculated with higher number of functions. The remaining three components are calculated with significantly smaller basis set (about three times smaller than for aug-pcJ-2_2006, see **Table 5**).

3.3. *Prediction of $^{1}J(^{15}N,H)$ in selected compounds*

Finally we calculated $^{1}J(^{15}N,H)$ coupling constants in the compounds in **Table 1** in chloroform and compared with experiment. Like for MSBTG, the B3LYP/6-311++G** geometry in $CHCl_3$ was used. First, for brevity, in **Table S4** in the Supplementary material we compared some technical details of calculations, including the number of atoms and basis functions. It is evident from **Table S4** that such molecules containing about 30 to 50 atoms can be easily calculated due to the fact that only one coupling between two spins is selected and predicted.

From **Table 5** it is evident that the pcJ-2 basis set is significantly larger than 6-311++G**(mixed) one. As seen from **Fig. 5**, using the APFD functional and 6-311++G** (mixed) basis set the coupling constants correlate very well with that obtained with pcJ-2 and considering that the latter basis overshoots the experimental values slightly and are computationally much more costly, the APFD/6-311++G**(mixed) functional/basis set seems to be a reasonable choice for predicting $^{1}J(^{15}N,H)$ coupling constants.

In **Table 6** are gathered $^{1}J(^{15}N,H)$ coupling constants for the studied molecules, compared with experiment and their deviations from experiment. For better illustration of the method performance, the deviations in % and the corresponding RMS values are also shown.

It is apparent from **Table 6** that indeed it is possible to predict fairly accurate $^{1}J(^{15}N,H)$ values in the studied set of molecules with a RMS value of 1.69 Hz. Thus, the calculated values overestimate experiment by only 1.91 %.

Plot of experimental vs. calculated $^{1}J(^{15}N,H)$ coupling constants for selected molecules is shown in **Fig. 6**. It shows that a fairly good correlation can be obtained between experimental and calculated $^{1}J(^{15}N,H)$ coupling constants leading to equation 1:

$$^{1}J(^{15}N,H)exp = 0.9128 * {}^{1}J(^{15}N,H)calc + 9.3763 \qquad \text{Eq. 1}$$

This enables to predict coupling constants rather accurately based on the calculation scheme mentioned above.

It is also important to investigate the dependence of calculated (predicted) $^{1}J(^{15}N,H)$ values with the calculated interatomic separation of coupled nitrogen and hydrogen atoms (spins). Thus, it is worth mentioning that theoretical modeling of N-H coupling constant magnitude vs. N...H distance reported Del Bene and Elguero[78-79]. On the other hand, Limbach et al.[6, 80-81] performed detailed experimental NMR studies on H-bonded systems.

As expected, it is apparent from **Fig. 7** that there is a linear dependence between the magnitude of calculated $^{1}J(^{15}N,H)$ value and the N-H bond length. Thus, by stretching the N-H bond (increasing H-bond interaction) a smaller absolute magnitude of coupling is predicted. This decrease of absolute magnitude of coupling constant is in agreement with chemical intuition. However, the FC term is dominating NH coupling (nearly 98%) and one could expect a more decaying exponential pattern with N...H distance.[78] Probably, because of a fairly small range of N-H distance changes the apparent linear result is observed from **Figure** 7.

A comparison of one-bond NH coupling constants of **10,** and **11** reproduces the experimental finding, that phenyl substitution at nitrogen leads to a smaller one-bond NH coupling constant.

From **Fig. 6** it is seen that the variation in $^{1}J(N,H)$ is less than 10 Hz. This of course requires experimental data with great precision (see Experimental) combined with some very accurately calculated values.

In tautomeric compounds like those shown in **Fig. 8** the measured coupling constant is a weighted average according to the mole fractions of the two forms.[5]

For tautomeric Schiff bases (**Fig. 8**) it was found that the XH chemical shift reaches a maximum corresponding to a $^{1}J(^{15}N,H)$ coupling constant of ~45 Hz.[6] Furthermore, X-ray data may suggest that the proton is positioned approximately midway between the acceptor and the donor atom[82]. The calculations of Zarycz and Aucar[18] show that the coupling constant at long bond distances is proportional to the NH bond length. . Using the equation between coupling constant and NH bond length derived in the present study (Fig. 7) a zero value is obtained at NH bond length of 1.23 Å, which is much closer than at the midpoint, which is estimated at 1.49 Å. This suggests that the proton is not in the centre at ambient temperature in

solution, but rather that an equilibrium is taking place leading to an average value of 45 Hz

To verify theoretically the dominating structure and proton (hydrogen) localization on N or O atom in the studied molecules we constructed a simple model molecule (**Fig. 9**) and performed a partial optimization mimicking H atom transfer from N to O atom.

Full optimization of NH and OH forms of the model molecule indicate that the former one is about 8.8 kcal/mol more stable in the gas phase. Since the NMR measurements for the studied molecules are performed in nonpolar solvent ($CDCl_3$ or CCl_4) a significant impact of environment could be ruled out. As the last step we decided to transfer proton from N to O freezing N5-H10 distance and optimizing all other parameters. Similarly, we moved H atom from oxygen toward N. Very small step of 0.02 Å near the energetic minima allowed determination of smooth energy curve and position of its fairly high barrier (9.9 kcal/mol for N-H distance of 1.32 Å). The corresponding energy landscape upon transfer from N to O atom of proton H10, taking part in H-bonding, is presented in **Fig. 10**.

It is obvious from **Fig. 10** that the global energy minimum corresponds to NH structure. Thus, modeling of proton H10 transfer one should observe a direct impact on the calculated $^{1}J(^{15}N,H)$ parameter of both protons attached to nitrogen atom. This is illustrated in **Fig. 11**.

Thus, increasing N-H(bond) distance from 0.9 to about 1.12 Å we observe a small and roughly linear decrease of calculated $^{1}J(^{15}N,H)$ and at higher separation a faster change is observed with saturation closer to the middle of N ... O distance. The corresponding N-H(free) coupling constant decreases linearly and very slowly to NH(bond) separation of about 1.12 Å and next diminishes faster and saturates at about -70 Hz.

It is apparent (**Fig. 10**) that the energy barrier to proton transfer is located between N and O atoms at N...H separation of about 1.35 Å. For this geometry the calculated coupling constant for H-bonded and free H atoms (**Fig. 11**) are -19.9 and -69.3 Hz. It is seen that the slope is much steeper for the hydrogen bonded than for the non-

hydrogen bonded N-H subunit. This supports the estimate above for the even stronger hydrogen bonded case that a zero coupling is found around 1.22 Å.

From **Figs. 10** and **11** it is apparent that the studied molecules, gathered in Table 1, show a diagnostic range of $^{1}J(^{15}N,H)$ coupling constant variation (from 94 to 86 Hz) despite the fact that the change in the calculated N-H separation is only from 1.020 to 1.036 Å (see **Fig. 7**).

With the trends derived for $^{1}J(^{15}N,H)$ we are able to explain why plots of $^{2}\Delta C(OD)$ vs. mole fraction for a range of *o*-hydroxy Schiff bases have maximum at slightly different mole fractions.[2, 4] These graphs were constructed using a common $^{1}J(^{15}N,H)$ value, leading probably to slightly incorrect mole fractions.

Having established a decent correlation between experimental and calculated $^{1}J(^{15}N,H)$ coupling constants one can predict values to be used for tautomeric systems in which the individual tautomers cannot be isolated. One example is the imine form of *E*-2-((1-phenylimino)ethyl)phenol (**1**) giving a $^{1}J(^{15}N,H)$calc as low as -81.2 Hz. Another example is the compound 8-Hydroxy-3,6dimethyl-2-(1-methylaminoethylidene)-2H=naphthalene-1-one, which is of C type. The coupling constant is measured at low temperature, $^{1}J(^{15}N,H)$ = 68 Hz[83]. This value is much lower than calculated, -91.87 Hz, indicating that the equilibrium not is shifted fully to the NH-form.

4. Conclusion

In summary, it can be said that $^{1}J(^{15}N,H)$ in Schiff bases and enaminones vary quite considerably taking into account tautomeric forms. Intramolecular hydrogen bonding is important as the NH bond length to some extent determines the magnitude of the one-bond NH coupling constant. The present finding for “enaminones” and Schiff bases are demonstrated to be valid also for other compounds with hydrogen bonded sp^2 hybridized nitrogens. The applied theoretical protocol, including B3LYP/6-311++G** structure optimization in chloroform within PCM approach and APFD/6-311++G**(mixed) calculation of $^{1}J(^{15}N,H)$ coupling constant well reproduces experimental NMR data for medium size organic molecules with intramolecular H-bond.

ASSOCIATED CONTENT

*sı Supporting Information

The Supporting Information is available free of charge at https://.

Authors

Poul Erik Hansen - Department of Science and Environment, Roskilde University, P.O.Box 260, DK-4000 Roskilde, Denmark, Fax +45 46743011, E-mail: poulerik@ruc.dk

Bahjat A. Saeed - Department of Chemistry, College of Education for Pure Sciences, University of Basrah, Iraq; E-mail: bahjat.saeed@yahoo.com

Rita S. Rutu - Department of Pharmaceutical Chemistry, College of Pharmacy, University of Basrah, Iraq

Teobald Kupka - University of Opole, Faculty of Chemistry, 45-052 Opole, Poland; orcid.org/0000-0002-6252-3822; Email: teobaldk@gmail.com

Declaration of competing interest

The authors declare no competing financial interest.

ACKNOWLEDGMENTS

We are grateful for a possibility of using hardware and software at Wrocław Supercomputing Center WCSS. T. K. is also grateful to the University of Opole for partial support during completing the study.

REFERENCES

[1] P. E. Hansen, in *Isotope effect in chemistry and biology*, ed. A. Kohen, H. H. Limbach. CRC Press, Taylor and Francis: Boca-Raton, F1, 2005.

[2] T. Dziembowska, Z. Rozwadowski, A. Filarowski, P. E. Hansen, *Magn. Reson. Chem.* **2001,** *39*, S67-S80.

[3] P. E. Hansen, J. Sitkowski, L. Stefaniak, Z. Rozwadowski, T. Dziembowska, *Ber. Buns. Gesell./Phys. Chem. Chem. Phys.* **1998,** *102*, 410-413.

[4] A. Filarowski, A. Koll, M. Rospenk, I. Krol-Starzomska, P. E. Hansen, *J. Phys. Chem. A* **2005,** *109*, 4464-4473, DOI: 10.1021/jp0445977.

[5] G. O. Dudek, E. P. Dudek, *J. Am. Chem. Soc.* **1966,** *88*, 2407-2412, DOI: 10.1021/ja00963a008.

[6] S. Sharif, G. S. Denisov, M. D. Toney, H. H. Limbach, *J. Am. Chem. Soc.* **2006,** *128*, 3375-3387, DOI: 10.1021/ja056251v.

[7] V. Macháček, A. Čegan, A. Halama, O. Rožňavská, V. Štěrba, *Collect. Czech. Chem. Commun.* **1955**, 1367-1379.

[8] L. Kozerski, K. Kamienska-Trela, L. Kania, W. Von Philipsborn, *Helv. Chim. Acta* **1983,** *66*, 2113-2128, DOI: 10.1002/hlca.19830660722.

[9] T. T. Quang, K. P. P. Nguyen, P. E. Hansen, *Magn. Reson. Chem.* **2005,** *43*, 302-308, DOI: 10.1002/mrc.1532.

[10] P. E. Hansen, Z. Rozwadowski, T. Dziembowska, *Curr. Org. Chem.* **2009,** *13*, 194-215, DOI: 10.2174/138527209787193738.

[11] A. Lyčka, D. Šnobl, *Collect. Czech. Chem. Commun.* **1981,** *46*, 892-897.
[12] M. Takasuka, Y. Terui *J. C. S. Perkin Trans. 2* **1984**, 1545-1550.
[13] M. Allen, J. D. Roberts, *J. Org. Chem.* **1980,** *45*, 130-135, DOI: 10.1021/jo01289a025.
[14] L. N. Kurkovskaya, R. N. Nurmukhametov, D. N. Shigorin, *Zh. Strukt. Khim.* **1980,** *21*, 61-70.
[15] R. E. Wasylishen, T. Schaefer, *Can. J. Chem.* **1973,** *51*, 3087-3096.
[16] T. Axenrod, P. S. Pregosin, M. J. Wieder, E. D. Becker, R. B. Bradley, G. W. A. Milne, *J. Am. Chem. Soc.* **1971,** *93*, 6536-6541, DOI: 10.1021/ja00753a035.
[17] Z. Rozwadowski, T. Dziembowska, *Magn. Reson. Chem.* **1999,** *37*, 274-278.
[18] N. Zarycz, G. A. Aucar, *J. Phys. Chem. A* **2008,** *112*, 8767-8774, DOI: 10.1021/jp802894f.
[19] J. B. Foresman, A. Frisch, *Exploring Chemistry with Electronic Structure Methods; Ed.* Second ed.; Gaussian Inc: Pittsburg, PA, 1996.
[20] M. J. Frisch, G. W. Trucks, H. B. Schlegel, G. E. Scuseria, M. A. Robb, J. R. Cheeseman, G. Scalmani, V. Barone, G. A. Petersson, H. Nakatsuji, X. Li, M. Caricato, A. V. Marenich, J. Bloino, B. G. Janesko, R. Gomperts, B. Mennucci, H. P. Hratchian, J. V. Ortiz, A. F. Izmaylov, J. L. Sonnenberg, D. Williams-Young, F. Ding, F. Lipparini, F. Egidi, J. Goings, B. Peng, A. Petrone, T. Henderson, D. Ranasinghe, V. G. Zakrzewski, J. Gao, N. Rega, G. Zheng, W. Liang, M. Hada, M. Ehara, K. Toyota, R. Fukuda, J. Hasegawa, M. Ishida, T. Nakajima, Y. Honda, O. Kitao, H. Nakai, T. Vreven, K. Throssell, J. A. Montgomery Jr., J. E. Peralta, F. Ogliaro, M. J. Bearpark, J. J. Heyd, E. N. Brothers, K. N. Kudin, V. N. Staroverov, T. A. Keith, R. Kobayashi, J. Normand, K. Raghavachari, A. P. Rendell, J. C. Burant, S. S. Iyengar, J. Tomasi, M. Cossi, J. M. Millam, M. Klene, C. Adamo, R. Cammi, J. W. Ochterski, R. L. Martin, K. Morokuma, O. Farkas, J. B. Foresman, D. J. Fox. Gaussian 16 Rev. B.01, Wallingford, CT, 2016.
[21] T. Kupka, M. Stachow, M. Nieradka, J. Kaminsky, T. Pluta, *J. Chem. Theory Comput.* **2010,** *6*, 1580-1589, DOI: 10.1021/ct100109j.
[22] W. Kohn, L. J. Sham, *Phys. Rev.* **1965,** *140*, A1133-A1138.
[23] J. K. Labanowski, J. W. Anzelm, *Density Functional Methods in Chemistry*. Springer-Verlag: New York, 1991.
[24] A. D. Becke, *Phys. Rev. A* **1988,** *38*, 3098–3100.
[25] C. Lee, Yang, W., and Parr, R. G., *Phys. Rev. B* **1988,** *37*, 785 - 789.
[26] B. Miehlich, A. Savin, H. Stoll, H. Preuss, *Chem. Phys. Lett.* **1989,** *157*, 200-206.
[27] R. Ditchfield, W. J. Hehre, J. A. Pople, *J. Chem. Phys.* **1971,** *54*, 724–728.
[28] W. J. Hehre, L. Radom, P. v. R. Schleyer, J. A. Pople, *Ab Initio Molecular Orbital Theory*. Wiley: New York, 1986.
[29] T. Enevoldsen, J. Oddershede, S. P. A. Sauer, *Theor. Chem. Acc.* **1998,** *100*, 275-284.
[30] T. Helgaker, M. Jaszunski, K. Ruud, *Chem. Rev.* **1999,** *99*, 293-352.
[31] T. Helgaker, M. Watson, N. C. Handy, *J. Chem. Phys.* **2000,** *113*, 9402-9409, DOI: 10.1063/1.1321296.
[32] F. Jensen, *J. Chem. Theory Comput.* **2006,** *2*, 1360-1369.
[33] P. F. Provasi, G. A. Aucar, S. P. A. Sauer, *J. Chem. Phys.* **2001,** *115*, 1324-1334.
[34] M. J. Frisch, G. W. Trucks, H. B. Schlegel, G. E. Scuseria, M. A. Robb, J. R. Cheeseman, G. Scalmani, V. Barone, B. Mennucci, G. A. Petersson, H. Nakatsuji, M. Caricato, X. Li, H. P. Hratchian, A. F. Izmaylov, J. Bloino, G. Zheng, J. L. Sonnenberg, M. Hada, M. Ehara, K. Toyota, R. Fukuda, J. Hasegawa, M. Ishida, T. Nakajima, Y. Honda, O. Kitao, H. Nakai, T. Vreven, J. Montgomery, J. A., J. E. Peralta, F. Ogliaro, M. Bearpark, J. J. Heyd, E. Brothers, K. N. Kudin, V. N. Staroverov, T. Keith, R. Kobayashi, J. Normand, K. Raghavachari, A. Rendell, J. C. Burant, S. S. Iyengar, J. Tomasi, M. Cossi, N. Rega, J. M. Millam, M. Klene, J. E. Knox, J. B. Cross, V. Bakken, C. Adamo, J. Jaramillo, R. Gomperts,

R. E. Stratmann, O. Yazyev, A. J. Austin, R. Cammi, C. Pomelli, J. W. Ochterski, R. L. Martin, K. Morokuma, V. G. Zakrzewski, G. A. Voth, P. Salvador, J. J. Dannenberg, S. Dapprich, A. D. Daniels, O. Farkas, J. B. Foresman, J. V. Ortiz, J. Cioslowski, D. J. Fox. Gaussian, Inc., Wallingford, CT, 2013.
[35] W. Deng, J. R. Cheeseman, M. J. Frisch, *J. Chem. Theory Comput.* **2006,** *2*, 1028-1037.
[36] N. F. Ramsey, *Phys. Rev.* **1953,** *91*, 303-307.
[37] L. B. Krivdin, *Progress Nucl. Magn. Reson. Spectr.* **2018,** *108*, 17-73, DOI: 10.1016/j.pnmrs.2018.10.002.
[38] L. B. Krivdin, *Prog. Nuc. Mag. Reson Sp.* **2018,** *105*, 54-99, DOI: 10.1016/j.pnmrs.2018.03.001.
[39] T. Helgaker, M. Jaszunski, M. Pecul, *Prog. Nucl. Magn. Reson.* **2008,** *53*, 249-268.
[40] L. B. Krivdin, R. Contreras, *Ann. Rep. NMR Spectrosc.* **2007**, 133-245.
[41] J. San Fabián, J. M. García De La Vega, R. Suardíaz, M. Fernández-Oliva, C. Pérez, R. Crespo-Otero, R. H. Contreras, *Magn. Reson. Chem.* **2013,** *51*, 775-787, DOI: 10.1002/mrc.4014.
[42] J. E. Peralta, G. E. Scuseria, J. R. Cheeseman, M. J. Frisch, *Chem. Phys. Lett.* **2003,** *375*, 452-458, DOI: 10.1016/S0009-2614(03)00886-8.
[43] T. Kupka, M. Nieradka, M. Stachow, T. Pluta, P. Nowak, H. Kjaer, J. Kongsted, J. Kaminsky, *J. Phys. Chem. A* **2012,** *116*, 3728-3738, DOI: 10.1021/jp212588h.
[44] H. Kjær, S. P. A. Sauer, J. Kongsted, *J. Chem. Phys.* **2010,** *133*, 144106, DOI: 10.1063/1.3483197.
[45] T. A. Ruden, O. B. Lutnaes, T. Helgaker, K. Ruud, *J. Chem. Phys.* **2003,** *118*, 9572-9581.
[46] A. Yachmenev, S. N. Yurchenko, I. Paidarová, P. Jensen, W. Thiel, S. P. A. Sauer, *J. Chem. Phys.* **2010,** *132*, 114305, DOI: 10.1063/1.3359850.
[47] P. Lantto, J. Vaara, T. Helgaker, *J. Chem. Phys.* **2002,** *117*, 5998-6009, DOI: 10.1063/1.1502243.
[48] G. O. Dudek, E. P. Dudek, *J. Am. Chem. Soc.* **1964,** *86*, 4283-4287.
[49] M. J. Frisch, G. W. Trucks, H. B. Schlegel, G. E. Scuseria, M. A. Robb, J. R. Cheeseman, G. Scalmani, V. Barone, G. A. Petersson, H. Nakatsuji, X. Li, M. Caricato, A. V. Marenich, J. Bloino, B. G. Janesko, R. Gomperts, B. Mennucci, H. P. Hratchian, J. V. Ortiz, A. F. Izmaylov, J. L. Sonnenberg, D. Williams-Young, F. Ding, F. Lipparini, F. Egidi, J. Goings, B. Peng, A. Petrone, T. Henderson, D. Ranasinghe, V. G. Zakrzewski, J. Gao, N. Rega, G. Zheng, W. Liang, M. Hada, M. Ehara, K. Toyota, R. Fukuda, J. Hasegawa, M. Ishida, T. Nakajima, Y. Honda, O. Kitao, H. Nakai, T. Vreven, K. Throssell, J. A. Montgomery Jr., J. E. Peralta, F. Ogliaro, M. J. Bearpark, J. J. Heyd, E. N. Brothers, K. N. Kudin, V. N. Staroverov, T. A. Keith, R. Kobayashi, J. Normand, K. Raghavachari, A. P. Rendell, J. C. Burant, S. S. Iyengar, J. Tomasi, M. Cossi, J. M. Millam, M. Klene, C. Adamo, R. Cammi, J. W. Ochterski, R. L. Martin, K. Morokuma, O. Farkas, J. B. Foresman, D. J. Fox. Wallingford, CT, 2016.
[50] J. Tomasi, B. Mennucci, R. Cammi, *Chem. Rev.* **2005,** *105*, 2999-3094, DOI: 10.1021/cr9904009.
[51] A. J. Cohen, N. C. Handy, *Mol. Phys.* **2001,** *99*, 607-615.
[52] J. P. Perdew, K. Burke, M. Ernzerhof, *Phys. Rev. Lett.* **1996,** *77*, 3865-3868.
[53] J. P. Perdew, K. Burke, M. Ernzerhof, *Phys. Rev. Lett.* **1997,** *78*, 1396.
[54] A. D. Becke, *J. Chem. Phys.* **1993,** *98*, 1372-1377.
[55] A. Austin, G. A. Petersson, M. J. Frisch, F. J. Dobek, G. Scalmani, K. Throssell, *J. Chem. Theory Comput.* **2012,** *8*, 4989-5007, DOI: 10.1021/ct300778e.
[56] S. P. A. Sauer, W. T. Raynes, *J. Chem. Phys.* **2000,** *113*, 3121-3129.

[57] V. Barone, P. F. Provasi, J. E. Peralta, J. P. Snyder, S. P. A. Sauer, R. Contreras, *J. Phys. Chem. A* **2003,** *107*, 4748-4754.
[58] Y. Y. Rusakov, L. B. Krivdin, S. P. A. Sauer, E. P. Levanova, G. G. Levkovskaya, *Magn. Reson. Chem.* **2010,** *48*, 44-52.
[59] P. F. Provasi, S. P. A. Sauer, *J. Chem. Phys.* **2010,** *133*, art. no. 054308.
[60] F. Jensen, *J. Chem. Theory Comput.* **2008,** *11*, 132-138
[61] B. P. Pritchard, D. Altarawy, B. Didier, T. D. Gibson, W. T. L., *J. Chem. Inf. Model.* **2019,** *59*, 4814-4820.
[62] K. L. Schuchardt, B. T. Didier, T. Elsethagen, L. Sun, V. Gurumoorthi, J. Chase, J. Li, T. L. Windus, *J. Chem. Inf. Model* **2007,** *47*, 1045-1052.
[63] D. Feller, *J. Chem. Phys.* **1992,** *96*, 6104 - 6114.
[64] D. Feller, *J. Chem. Phys.* **1993,** *98*, 7059 - 7071.
[65] M. W. Feyereisen, Feller, D., Dixon, D. A., *J. Phys. Chem.* **1996,** *100*, 2993-2997.
[66] T. Kupka, B. Ruscic, R. E. Botto, *J. Phys. Chem. A.* **2002,** *106*, 10396-10407.
[67] T. Kupka, C. Lim, *J. Phys. Chem. A* **2007,** *111*, 1927-1932.
[68] T. Helgaker, W. Klopper, H. Koch, J. Noga, *J. Chem. Phys.* **1997,** *106*, 9639 - 9646.
[69] T. H. Dunning, Jr., *J. Chem. Phys.* **1989,** *90*, 1007-1023.
[70] R. A. Kendall, T. H. Dunning, Jr., R. J. Harrison, *J. Chem. Phys.* **1992,** *96*, 6796 - 6806.
[71] D. E. Woon, and Dunning, T. H.. Jr., *J. Chem. Phys.* **1993,** *98*, 1358 - 1371.
[72] F. Jensen, *J. Chem. Phys.* **2001,** *115*, 9113 - 9125.
[73] F. Jensen, *J. Chem. Phys.* **2003,** *118*, 2459 - 2463.
[74] R. E. Wasylishen, J. O. Friedrich, *Can. J. Chem.* **1987,** *65*, 2238-2243.
[75] R. M. Gester, H. C. Georg, S. Canuto, M. C. Caputo, P. F. Provasi, *J. Phys. Chem. A* **2009,** *113*, 14936-14942.
[76] T. Kupka, *Magn. Reson. Chem.* **2009,** *47*, 959-970.
[77] S. Ullah, W. Zhang, P. E. Hansen, *J. Mol. Struct.* **2010,** *976*, 377-391, DOI: 10.1016/j.molstruc.2010.03.059.
[78] J. E. Del Bene, J. Elguero, *J. Phys. Chem. A* **2006,** *110*, 7496-7502, DOI: 10.1021/jp0613642.
[79] J. E. Del Bene, J. Elguero, *J. Am, Chem. Soc.* **2004,** *126*, 15624-15631, DOI: 10.1021/ja0401545.
[80] H.-H. Limbach, M. Pietrzak, S. Sharif, P. M. Tolstoy, I. G. Shenderovich, S. N. Smirnov, N. S. Golubev, G. S. Denisov, *Chem. Eur. J.* **2004,** *10*, 5195-5204, DOI: 10.1002/chem.200400212.
[81] P. M. Tolstoy, S. N. Smirnov, I. G. Shenderovich, N. S. Golubev, G. S. Denisov, H.-H. Limbach, *J. Mol. Struct.* **2004,** *700*, 19-27.
[82] A. Filarowski, *J. Phys. Org. Chem.* **2005,** *18*, 686-698, DOI: 10.1002/poc.940.
[83] P. Madelung, J. C. Scönbeck, A. Lund. Thesis. Roskilde University, 2004.

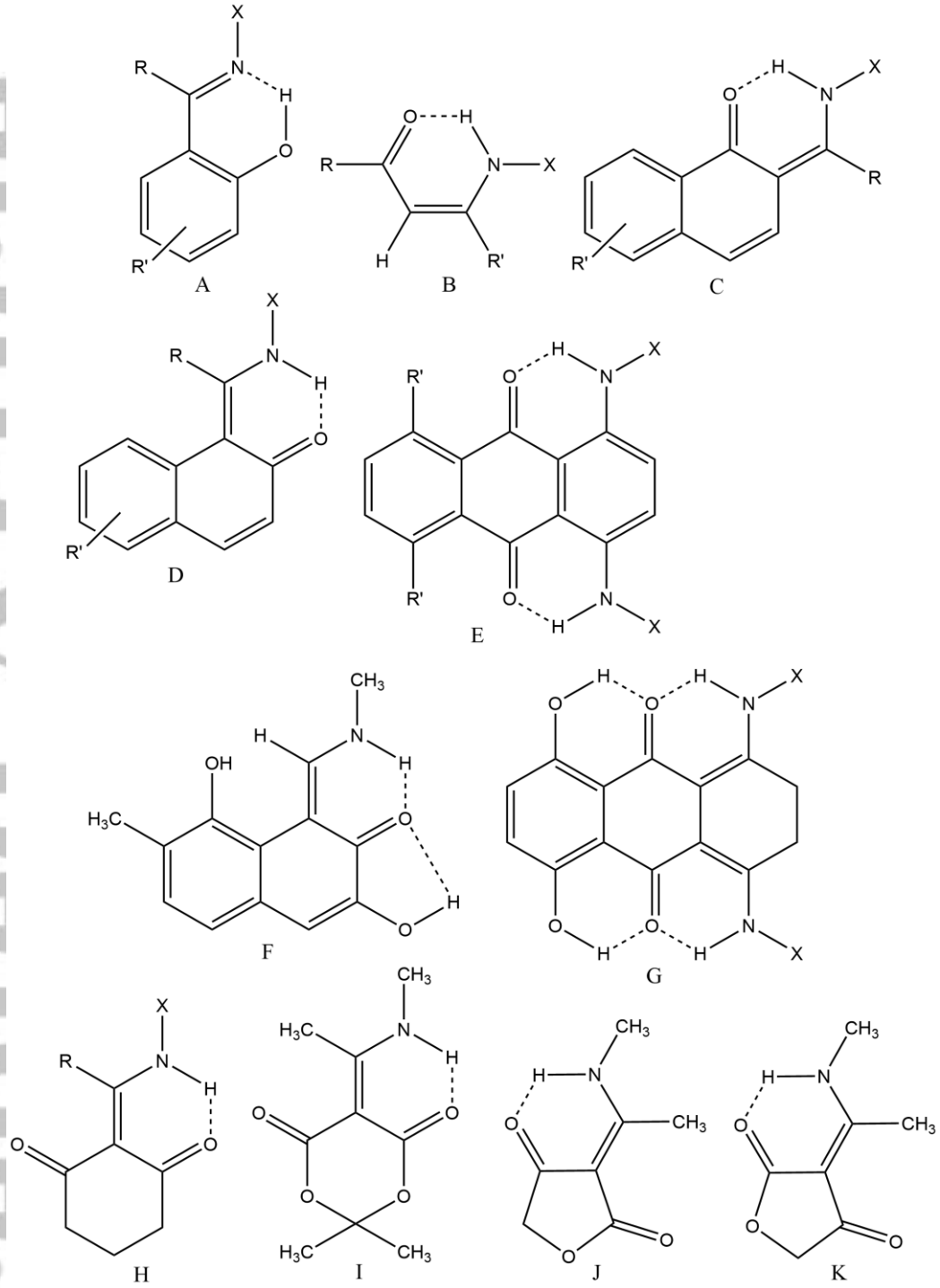

Fig. 1. Structures (A – K) of calculated compounds

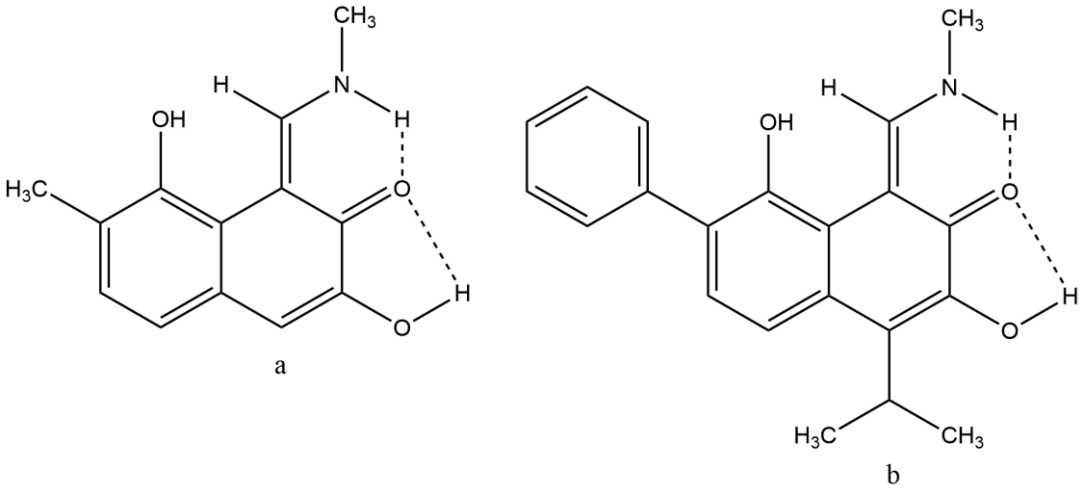

Fig. 2. Methyl amine Schiff bases of truncated forms (**a** and **b**) of gossypol. Structure "**a**" is MSBTG.

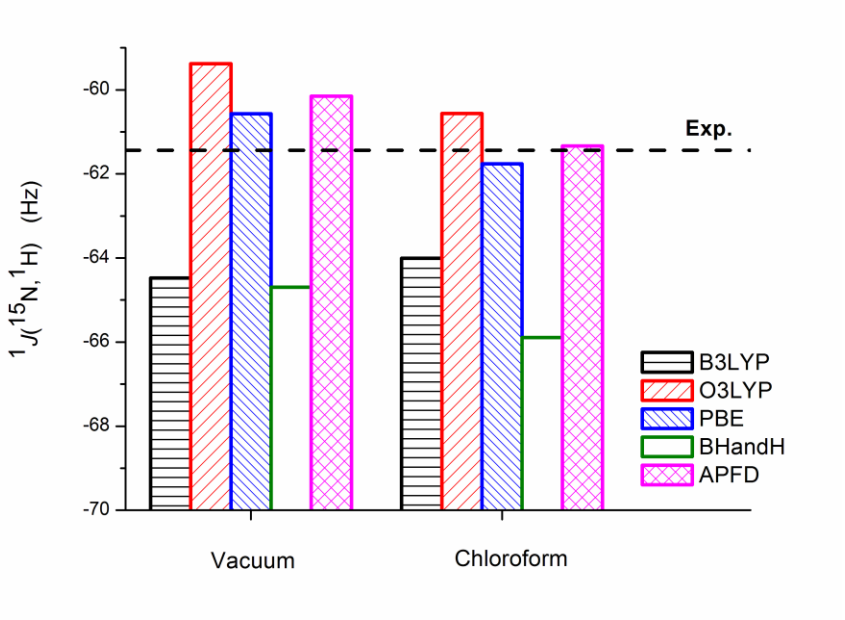

Fig. 3. Performance of B3LYP, O3LYP, PBE, BHandH and APFD density functionals in prediction of $^1J(^{15}N,H)$ in ammonia in vacuum and chloroform. Experimental[74] values are marked as dashed lines. 6-311++G**(mixed) basis set was used for SSCC calculations.

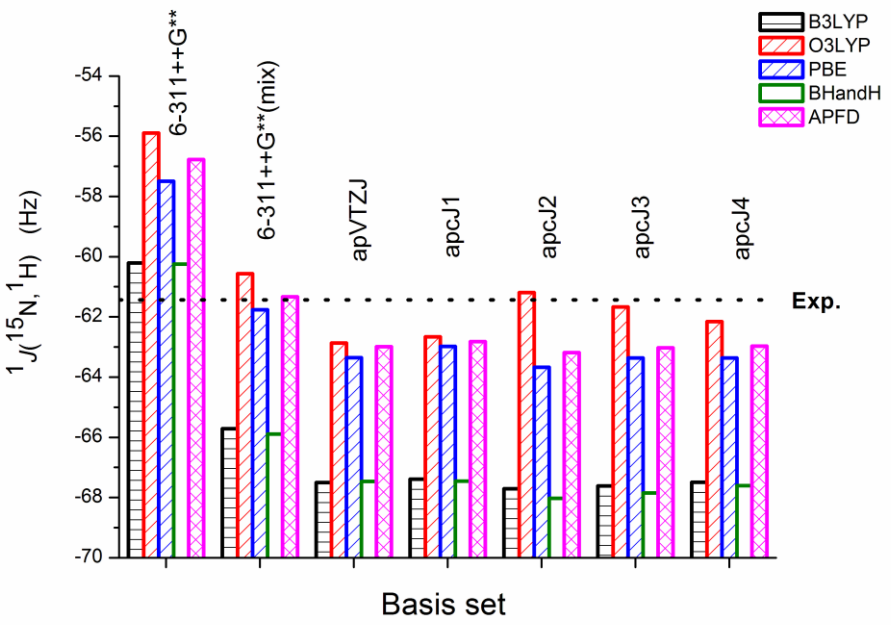

Fig. 4. Comparison of $^1J(^{15}N,H)$ for ammonia in chloroform, calculated with five selected density functionals and basis sets with experimental value.

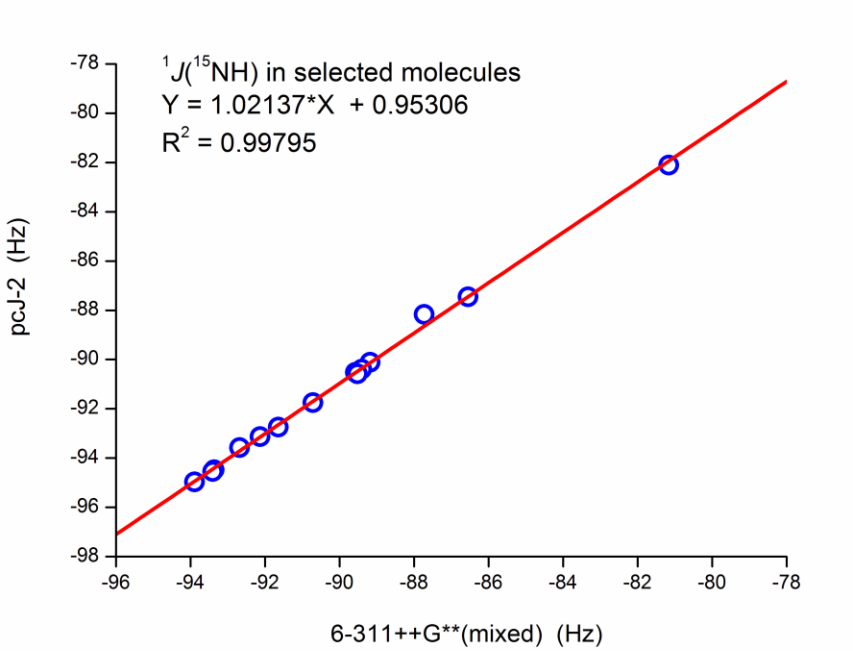

Fig. 5. A plot of APFD predicted $^1J(^{15}N,H)$ by pcJ-2 vs. 6-311++G**(mixed) basis sets for selected compounds in $CHCl_3$. B3LYP/6-311++G** in $CHCl_3$ optimized structures are used

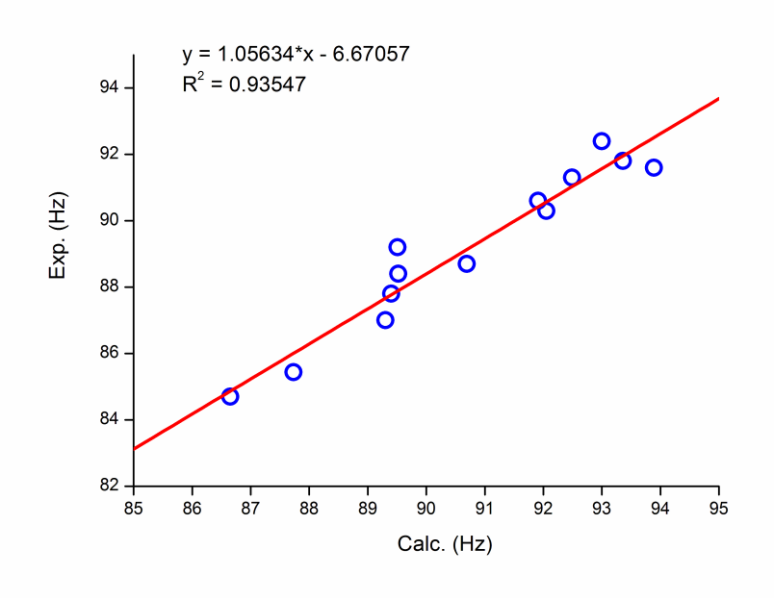

Fig. 6. Plot of experimental *vs.* theoretical APFD/6-311++G**(mixed) calculated $^{1}J(^{15}N,H)$ coupling constants for selected molecules at their B3LYP/6-311++G** geometries in $CHCl_3$

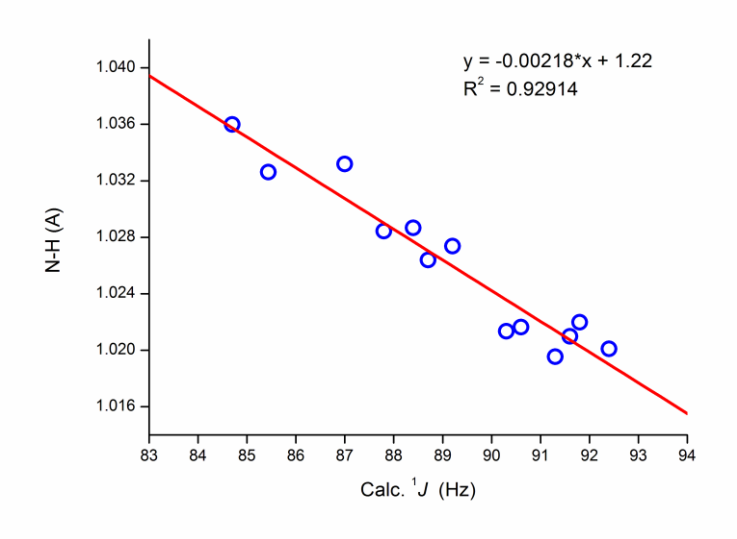

Fig. 7. Linear dependence between NH bond length and calculated $^{1}J(^{15}N,H)$ coupling constant

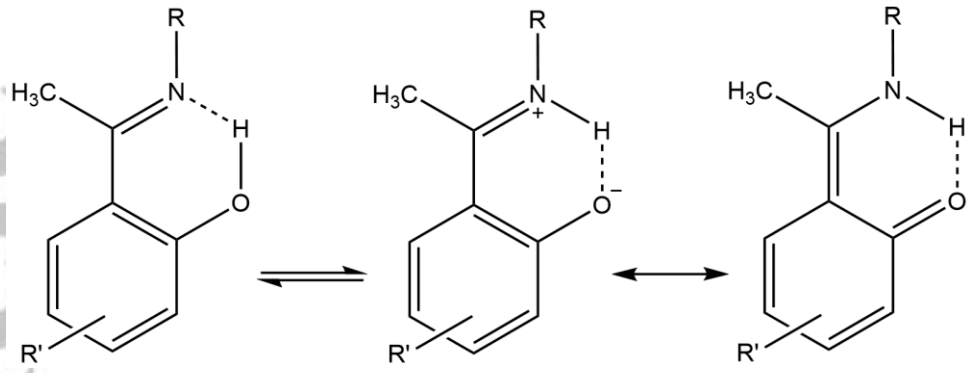

Fig. 8. Tautomeric and resonance forms of *o*-hydroxy Schiff bases

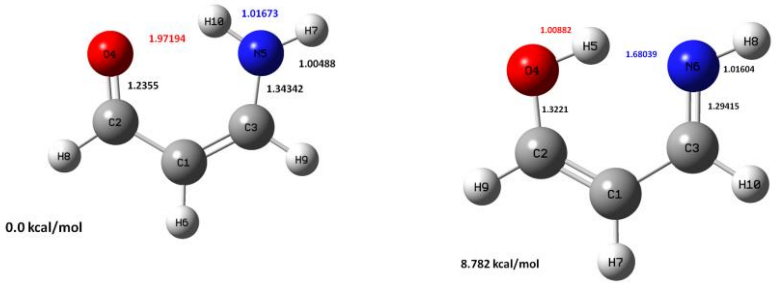

Fig. 9. (*Left*) NH and (right) OH forms of tested model molecule with atom numbering, selected interatomic distances and relative stability (result from full B3LYP/6-311++G** optimization in vacuum).

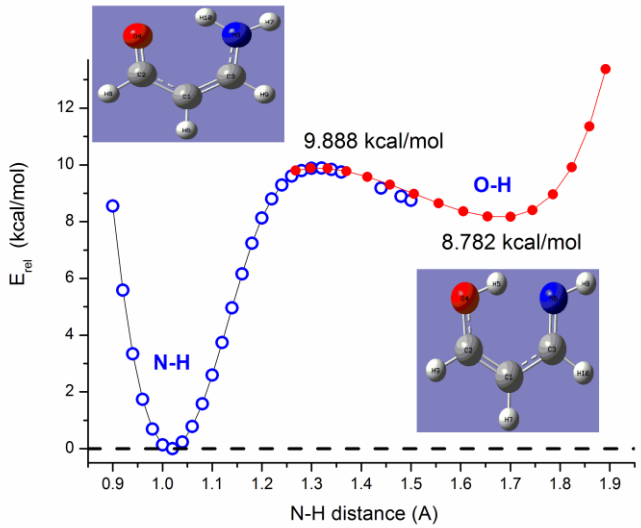

Fig. 10. Energy landscape upon proton H10 transfer from N to O atom. Relative stability of NH and OH forms are given and the barrier height is also marked.

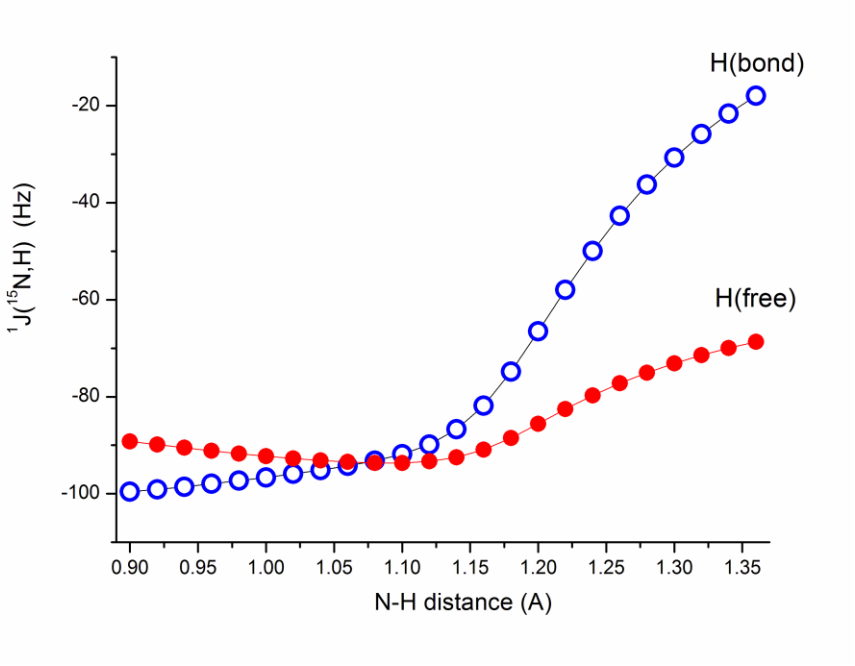

Fig. 11. Sensitivity of $^1J(^{15}N,H)$ to H10 proton transfer. Separate coupling constants are shown for H atom taking part in H-bonding and the other one (APFD/6-311++G**(mixed) is used for SSCC calculation.

Table 1. Compounds investigated.

Cmpd	R [a]	R´	X	Names
1	CH_3	H	Ph	(E)-2-((1-(phenylimino)ethyl)phenol (A)
2	Ph	CH_3	CH_3	3-Methylamino-1-phenyl-but-2-en (B)
3	Ph	CH_3	Ph	1-Phenyl-3-phenylamino-but-2-en-1-one (B)
4	H	H	tbu	(E-)1-(t-butylamino)-naphthalene-2-ol (D)
5	H	H	Ph	(E)-1-((phenylimino)methyl)naphthalen-2-ol (D)
6	-	H	Ph	1,4-di-(phenylamino)-9,10-anthraquinone (E)
7	-	OH	Ph	1,4-di-(phenylamino)-5,8-dihydroxy-9,10-anthraquinone (E)
8	-	-	-	Methylamine Schiff base of "gossypol" a (F) [b], MSBTG
9	-	-	CH_3	5,8-Dihydroxy-1,4-bis-phenylamino-2,3-dihydro-anthraquinone (G)
10	CH_3	-	CH_3	2-(1-(methylamino)ethylidene)cyclohexane-1,3-dione (H)
11	CH_3	-	Ph	2-(1-(phenylamino)ethylidene)cyclohexane-1,3-dione (H)
12	-	-	-	2,2-dimethyl-5-(1-(methylamino)ethylidene)-1,3-dioxane-4,6-dione (I)
13	-	-	-	(E)-3-(1-methylamino)ethylidene)furan-2,4(3H,5H)-dione (J)
14	-	-	-	(Z)-3-(1-methylamino)ethylidene)furan-2,4(3H,5H)-dione (K)

[a] The letters refer to Fig. 1; [b] See Fig. 2

Table 2. Relative content (in %) of four individual components of total $^1J(^{15}N,H)$ in MSBTG calculated with B3LYP density functional combined with standard and mixed 6-31G* and 6-311++G** basis sets in the gas phase and chloroform.

SSCC components	Gas		$CHCl_3$	
	Standard	Mixed	Standard	Mixed
6-31G*[a]				
FC	97.77	98.07	97.78	98.08
SD	0.26	0.23	0.27	0.24
PSO	1.31	1.13	1.29	1.12
DSO	0.66	0.57	0.64	0.56
6-311++G**[b]				
FC	97.92	98.14	97.88	98.10
SD	0.45	0.40	0.47	0.42
PSO	1.02	0.91	1.06	0.95
DSO	0.61	0.54	0.60	0.54

[a] Using B3LYP/6-31G* geometry in the gas phase and chloroform, respectively; [b] Using B3LYP/6-311++G** geometry in the gas phase and chloroform, respectively

Table 3. Impact of geometry on $^{1}J(^{15}N,H)$ in MSBTG [a], calculated with B3LYP density functional (both geometry and SSCC calculated at the same level of theory).

Method and Basis	Basis Type	Vacuum			Chloroform		
		$^{1}J(^{15}N,H)$	Dev.	% Dev.	$^{1}J(^{15}N,H)$	Dev.	% Dev.
6-31G*	Mixed	-94.47	5.76	6.50	-94.14	5.44	6.13
6-311++G**	Mixed	-95.57	6.87	7.74	-95.42	6.72	7.58
6-311++G(3df,2pd)	Mixed	-95.12	6.42	7.23	-94.81	6.11	6.89
Exp.[b]		**88.7**					

[a] No ZPVC. Dev = Calc – Exp; %Dev = 100*Dev/(88.7); [b] From ref. [9]

Table 4. $^{1}J(^{15}N,H)$ in MSBTGl[a,b] calculated with B3LYP and BHandH density functionals in chloroform, using selected "mixed" Pople-type basis sets and standard pcJ-2.

Method and Basis	Basis type	Chloroform		
		$^{1}J(^{15}N,H)$	Dev.	% Dev.
B3LYP				
6-31G*	Mixed	-94.09	5.39	6.08
6-311++G**	Mixed	-95.03	6.33	7.14
6-311++G(3df,2pd)	Mixed	-94.81	6.11	6.89
pcJ-2	Original	-96.16	7.46	8.41
BHandH				
6-31G*	Mixed	-94.26	5.56	6.27
6-311++G**	Mixed	-94.97	6.27	7.06
6-311++G(3df,2pd)	Mixed	-94.59	5.89	6.64
pcJ-2	Original	-96.17	7.47	8.42
Exp.[c]		**88.7**		

[a] B3LYP/6-311++G(3df,2pd) optimized geometry in chloroform; [b] Dev = Calc – Exp; %Dev = 100*Dev/(88.7). [c] Experimental value from ref. [9]

Table 5. $^{1}J(^{15}N,H)$ in MSBTG [ab], calculated with B3LYP and APFD density functionals in chloroform, using selected "mixed" Pople-type basis sets and standard pcJ-2 and aug-pcJ-2_2006 basis sets.

Basis set	No b.f.	$^{1}J(^{15}N,H)$	From Exp	
			Dev.	**%Dev**
B3LYP in $CHCl_3$				
6-311++G**	465	-85.29	3.41	-3.84
6-311++G**(mixed)	798	-95.04	-6.34	7.14
pcJ-2	1179	-96.16	-7.46	8.41
APFD in $CHCl_3$				
6-311++G**	465	-81.85	6.85	-7.72
6-311++G**(mixed)	798	-90.35	-1.65	1.86
pcJ-2	1179	-91.39	-2.69	3.03
Aug-pcJ-2_2006	1568	-92.51	-3.81	4.29
Exp. [c]		**-88.7**		

[a]Dev = Calc – Exp and Calc. – Emp., respectively; %Dev = 100*Dev/(Exp.) and 100*Dev/(Emp.), respectively; [b]Structures calculated at B3LYP/6-311++G(3df,2pd) level of theory; [c] From ref. [9]

Table 6. $^{1}J(^{15}N,H)$ predicted by APFD/6-311++G**(mixed) calculations for selected compounds in $CHCl_3$ (geometry also optimized in $CHCl_3$ at B3LYP/6-311++G** level of theory). Deviation from experiment (in Hz and %) as well as the corresponding RMS values are shown.

Molecule	**Exp.**	**$^{1}J(^{15}N,H)$**	**Dev. from Exp**	
Symbol			**Dev.**	**%Dev**
2	-91.6 [a]	-93.89	-2.29	2.50
3	-89.2[b]	-89.57	-0.37	0.41
4	-85.44[c]	-87.73	-2.29	2.68
5	-87[d]	-89.18	-2.18	2.51
6	-90.3[e]	-92.13	-1.83	2.03
7	-91.3 [e]	-92.68	-1.38	1.51
8	-88.7[f]	-90.71	-2.01	2.27
9	-87.8[e]	-89.40	-1.6	1.82
10	-88.1[g]	-89.52	-1.42	1.61
11	-84.7 [h]	-86.55	-1.85	2.18
12	-90.6 [i]	-91.64	-1.04	1.15
13	-91.8[i]	-93.36	-1.56	1.70
14	-92.4[i]	-93.40	-1	1.08
RMS			1.69	1.91

a) Ref. [48]; b) Ref. [48]. Measured at 253 K; c) Ref. [2]. Measured at 243K; d) Phenol is added to force the equilibrium fully towards the NH-form. Measured at 213K. Ref. [14]; e) Ref. [11]. Measured at 300 K; f) Measured in THF-d_8 at 298K. Ref. [9]; g) Ref. [48]. Measured at 245 K; h) Ref. [5]. Measured at 243 K; i) Ref.[77]. Measured at 298 K.

Graphical abstract

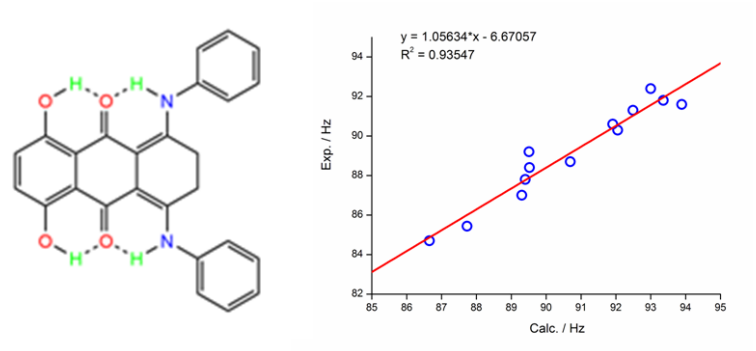

Theoretical *vs.* experimental $^{1}J(^{15}N,H)$ coupling constants for selected molecules.